Smart, Wearable and Power-Controlled Mixed-Signal Platform for Screening and Follow-up of Cystic Fibrosis based on Real-Time Chloride Concentration Evaluation in Sweat

Smart, Wearable and Power-Controlled Mixed-Signal Platform for Screening and Follow-up of Cystic Fibrosis based on Real-Time Chloride Concentration Evaluation in Sweat

Daniela De Venuto[1], *IEEE Member*, Grazia Mascellaro[1], Giuseppe Spadavecchia[1], Domenica De Venuto[2], Paolo Bollella[3], Luisa Torsi[3]

[1]Politecnico di Bari, Dip. di Ingegneria Elettrica e dell'Informazione, Bari, Italy
daniela.devenuto@poliba.it
[2] Azienda Ospedaliero Universitaria Consorziale Policlinico, Bari, Italy
[3] Dipartimento di Chimica, Università degli Studi di Bari Aldo Moro, Bari, Italy

***Abstract*— The paper presents a fully integrated wearable sensing system for real-time monitoring of chloride concentration in human stimulated perspiration, allowing accurate cystic fibrosis detection and follow-up monitoring. To improve wearability and comfort, fully flexible support has been employed for both the electrodes and the smart electronics. Novel design and manufacture for the ion-sensitive electrodes are here proposed, demonstrating Nernstian sensitivity in chloride concentration detection. The developed smart mixed-signal electronic platform embeds an analog read-out performing potentiometric measurements and digital section including a microcontroller and RF interface. This last section deals with the automation of sweat test processes, data processing, and the generation of suggestions to support diagnostics. The whole architecture is here described with emphasis on the power-management to achieve an extremely low power consumption and also on the capability of the system to allow a reasoning on the measured data and on the history of the patient. Finally, a case study based on experimental results is here reported, demonstrating the feasibility of the system, which can be comfortably worn due to its size, flexibility, and the biocompatibility of the materials used.**

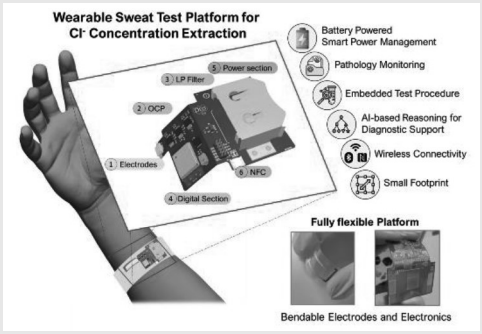

***Index Terms*— Potentiometry, wearable chloride biosensing, readout electronics for electro-chemical sensing, electrodes, Cystic Fibrosis screening and diagnosis.**

I. INTRODUCTION

WEARABLE sensors have earned great interest in recent years, especially in the field of personalized diagnosis and healthcare tracking [1]. This is because some biological and physiological parameters require continuous monitoring to assess health status of the patients undergoing novel drug-based therapies.

In the last two decades, extensive research has been conducted to develop comfortable-to-use devices, leading to the creation of various portable systems with different geometries, sizes, and materials [2].

Some important parameters that are interesting to be monitored to deduce information about the subject's health-conditions and first symptoms of disorders are: endogenous compounds, e.g., lactate and glucose and ions, e.g., Na^+, K^+ and Cl^- ([3- 5]). The endogenous compounds reveal the status of the metabolism of the organism, while ions give indication of the body hydration, heat-stress, bone composition, etc.

All these compounds change their concentration depending on the body fluids where they are detected: (i) blood, (ii) saliva, (ii) urine or (iv) skin excretion, such as sweat.

Sweat can be defined as an optimal fluid to monitor metabolites and ions since it is non-invasive, whereas blood requires the insertion of catheters or the use of implantable sensors [5]. In Cystic Fibrosis (CF) the sweat test is the screening procedure [6]. CF is caused by mutations in the cystic fibrosis transmembrane conductance regulator (CFTR) gene that affects the production of the CFTR protein. When the CFTR protein is not made correctly, it affects the balance of salt and fluids inside and outside of the cell. This imbalance leads to thick, sticky mucus in the lungs, pancreas, and other organs [7].

For the diagnosis of CF, the sweat test is considered the gold standard test and must be performed by trained personnel with a lot of experience, to guarantee the correct application of the guidelines for the correct execution and interpretation of the Sweat Test [7,8]. The sweat test is mandatory before the third month of life and later once the diagnosis of CF is done, should

be repeated in subjects of any age in case of therapeutical follow-up, with specific therapy, following the agenda given by the drug company, responsible of the possible drawbacks.

The test consists in determining the concentration of chloride in sweat. In the first part of the test, sweating is induced in a small area of the forearm with pilocarpine iontophoresis. This stage takes about 5 minutes. The iontophoresis can induce an itchy sensation in the patient and sometime low amount of sweat that invalidate the result. The sweat is collected either on a blotting paper, otherwise on a cardboard, or on a gauze and even through a small plastic tube wound in a spiral. This phase lasts 30 minutes. The collected sweat is then sent to the laboratory to measure the chlorine concentration. The technical time for this measurement is half a day if the laboratory is on site, otherwise, typically the waiting should not exceed two days.

The first condition necessary to consider a suitable sweat sample is the amount of sweat collected which must not be less than 75 mg if collected on paper/gauze or 20 μl if collected with plastic coils. In some centers, sweat testing is performed with collection from both forearms and separate analysis of the two samples. The agreement of the values between the two tests reinforces the reliability of the result, representing a useful control of the method. Chloride is the analyte that best correlates with the basic defect of this disease, i.e., the lack or malfunction of the CFTR protein, a protein that is mainly responsible for the transport of chloride ions at the of epithelial tissues [7]. The numerical result of the test, i.e., the concentration of chloride in the sweat, must always be accompanied by an adequate analytical interpretation and by comment from the clinician as the diagnosis of cystic fibrosis constitutes a medical act. Today, pharmaceutical treatments for cystic fibrosis are available and are composed of modulators of the CFTR protein. They have demonstrated a very significant efficacy in improving respiratory and nutritional conditions and quality of life in subjects with cystic fibrosis. In the last two years drugs that target specific defects in the CFTR protein have been developed and clinical trials are on-going even starting to be used to treat children from 6 months, or 2 years or 7 years in dependence on the drug formula. As a group, these drugs are called modulators because they are intended to modulate the function of the CFTR protein so that it can serve its primary function: to create a channel for chloride to flow across the cell surface.

When proper chloride flow is reestablished, mucus becomes rehydrated inside the lungs and other organs. Although modulators can't yet completely restore proper chloride flow, they can improve the flow enough to relieve symptoms for people with CF.

For all the time of the treatment, the patient should be monitored to be sure of the effectiveness of the treatment. The majority of patients demonstrated an improvement in respiratory and nutritional parameters and a decrease in sweat test values. Inside the centers where the treatment is suggested, the number of sweat test increases exponentially.

The focus of our proposal is to make easy and comfortable the sweat test for the CF patients such that they can check the successful progress of the therapy at home, under medical control.

At this aim, we have considered key factors like the combination of wireless connectivity (Bluetooth Low-Energy), wearability, substrate flexibility, small dimensions to fit in an armband, and low-power consumption during the device realization. The replaceable electrodes for the potentiometric extraction of the chloride concentration together with the electronic readout have been potentiated by the capability of the microcontroller to perform a reasoning on the data deriving, in real-time, diagnosis support for the medical doctor.

The paper is organized as follows. Sec. II outlines the architecture of the device, providing design details and experimental measurements about the read-out electronics, digital and RF section (microcontroller and interfaces). Sec. II also provides an overview of the functionalities implemented by the firmware used for data analysis and onboard devices control. Sec. III presents a case study with experimental results to offer a more comprehensive description of the workflow of the proposed device. Section IV concludes the paper.

II. The Wearable Analyzer of Chlorine Concentration in Sweat

Figure 1 illustrates the architectural layout of the proposed wearable sweat analyzer, depicting a potential mode of operation of the device during neonatal CF screening. The portable sweat test tool consists of two distinct components: (i) the electrodes; (ii) the electronic detection and analysis device. The electrodes are designed to be disposable, flexible, and replaceable. They are connected to the electronics through a zero-insertion force (ZIF) connector, ensuring exposure of the active sensing area in contact with the skin. The electronics, implemented on a flexible substrate, is reusable for all measurements.

The sweat analyzer is designed to be compact and fully bendable, allowing the electrodes and connected electronics to adapt to a wide range of curvature, making them integrable within a bracelet to be fastened to the subject's forearm. Once the device is properly positioned, the detection system: (i) autonomously initiates the sweat test procedures; (ii) stores data for the subject's history; (iii) transmits results to a Fast Healthcare Interoperability Resources (FHIR) server; (iv) provides diagnostic support by transmitting recommendations for the proper procedure; (v) enables automatic scheduling of tests in accordance with the selected therapy.

As depicted in Figure 1, the architecture comprises five primary blocks: (i) Electrodes; (ii) OCP; (iii) LP Filter; (iv) Microcontroller (μC) and (v) Power Supply.

The electrodes establish the interface with the skin for the proposed sensing system, realizing an electrochemical sensor sensitive to the concentration of Cl^- in the sweat sample within the active area. The two electrodes are the reference electrode (RE) and the sensing electrode, also known as the working electrode (WE). The first stage of the electronics is the Open Circuit Potential (OCP) block, which is responsible for implementing the potentiometric technique by reading the voltage drop between the WE and RE. The OCP block is followed by a signal filtering stage (LP filter), which aims to reduce noise outside the bandwidth of interest for the specific

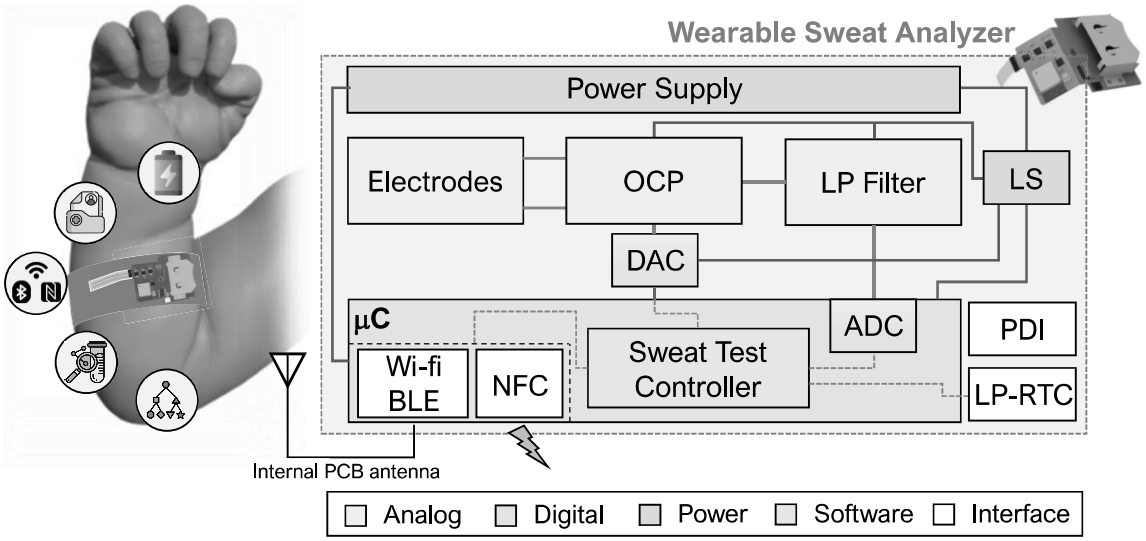

Fig. 1. Block diagram representation of the proposed wearable sweat analyzer

application.

The filtered signal at the output of the analog front-end is then connected to a µC-embedded Analog-Digital Converter (ADC). The ADC is controlled by the software named Sweat Test Controller in Figure 1, which runs on the microcontroller. This software is responsible for scheduling measurements, analyzing them, and transmitting results and clinical suggestions through the Bluetooth Low Energy (BLE)/WiFi (or both) interface to a dedicated gateway. The software also controls the Digital-Analog Converter (DAC) regulating the offset of the OCP block for waveform centering the ADC's dynamic range.

The Power Supply block consists of the main power source (coin battery), the voltage regulator and the load switch controlled by the microcontroller to deactivate the analog front-end once the measurements are completed.

The introduction of an integrated heater in the electrode section is under investigation. It will have the purpose of thermally stimulating localized eccrine sweat production on the forearm, without the need to use pilocarpine and subsequent iontophoresis.

A. The Electronics

1) *Flexible Printed Circuit Board*

The wearable sweat analyzer electronics is realized through a flexible Printed Circuit Board (FlexPCB) manufactured with a 0.3mm Polyimide (PI) substrate. The complete FlexPCB has a size of 49.4 mm × 39.5 mm, but smaller versions without debug and NFC interfaces, or reduced OCP readout are available. Figure 2 shows a snapshot of the complete FlexPCB. In Figure 2a, it can be possible to identify: (i) the first stage of OCP (#2 - Figure 2.a); (ii) the LP filter stage (#3 - Figure 2.a); (iii) the Digital Section (#4 - Figure 2.a), which includes a microcontroller (µC), debug interface, NFC connection (#6 - Figure 2.a), and (iv) the Power Section (#6 - Figure 2.a), which includes the power source (battery), a linear regulator, and a load switch.

2) *First Stage: OCP*

The first stage of the Analog Front-End (AFE) is the block referred to as OCP in Figure 1. The OCP technique implies negligible current condition between the two electrodes [9]. The first sensor interface stage has been implemented by connecting two high-impedance voltage buffers to the electrodes (Figure 3). The operational amplifiers U1 and U2 responsible for creating the buffer stage are MAX44242 by Analog Devices. The MAX44242 shows high input impedance (200 GΩ) and extremely low input bias current (max 0.5 pA). The open loop gain (A_{OL}) is 145 dB and the low input offset is of 50µV, with temperature drift of ±0.25µV/°C w.r.t. 25 °C.

The buffered potentials, V_{WE} and V_{RE}, are then routed to a differential stage, U3, through resistors R_1 and R_2, while resistor R_4 is used for gain management.

In this design, $R_1 = R_2 = R_4$, to get an unity gain. The R_3 is used to add offset voltage V_{OS} to the difference between V_{WE} and V_{RE}.

V_{OS} is controllable through a DAC with buffered output. The management of the V_{OS} is handled by the µC. More details concerning V_{OS} management are provided in Sec. II.B The U3 is a MAX4477 by Analog Devices. The MAX4477 is configured as unity-gain stable amplifier with low distortion.

It exhibits good DC characteristics, with an A_{OL} of 110 dB and an input offset voltage of 70 µV with a temperature drift of ±0.3 µV/°C with respect to 25°C. The MAX4477 has an input bias

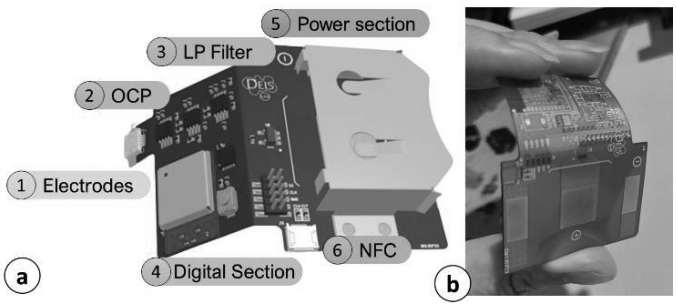

Fig. 2. Wearable sweat analyzer FlexPCB. (a) 3D rendering with identified sections; (b) Realized FlexPCB

current of 1 pA (max), which does not introduce significant additional offset errors on the input resistors.

The device features are: a high differential input impedance (1 TΩ) and a low output impedance (0.2 Ω @ 200 Hz - 2 Ω @ 1 kHz with Av=+1).

The noise budget of the front-end stage is summarized in Table 1. Table 1 provides the noise figure extracted from the datasheets of the involved devices, divided into three main noise bands (i.e., 0.1-10 Hz, 1/f noise, and broadband noise). Specifically, the 1/f noise also includes the noise corner frequency (f_{nc}). The second part of Table 1 presents the noise budget under reported operating conditions. The bandwidth (BW) value chosen is fixed at 200 Hz with a 4-pole correction associated with the filtering stage selection detailed in the following paragraph.

In terms of the power budget, both the MAX44242 and the MAX4477 are operated in a single-supply configuration with a voltage of +3.3V. The MAX44242 draws a current of 1.2 mA per amplifier (the MAX44242 package contains two amplifiers), whereas the MAX4477 consumes 2.2 mA.

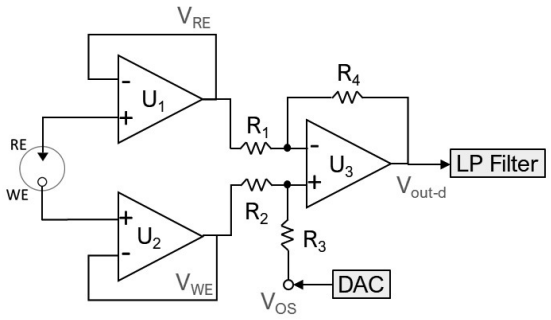

Fig. 3. Simplified schematic of AFE for the electrodes front-end.

TABLE I
NOISE BUDGET OCP STAGE

Device	0.1 Hz -10 Hz noise	1/f noise (input voltage noise density) [nV/√(Hz)]	Broadband noise (input voltage noise density) [nV/√(Hz)]
MAX44242	1.6 μVpp	f_{nc}=1235 Hz 35 @ 10 Hz 5 @ f_{nc}	5
MAX4477	260 nVpp	f_{nc}=865 Hz 21 @ 10 Hz 5 @ f_{nc}	4
Noise Budget			
Conditions		**$E_{n\text{-}tot}$ OCP**	
T = 25 °C, R1..4=100kΩ, G=+1 BW= 200 Hz (4th ord. correction)		$E_{n\text{-}tot,in}$ = $E_{n\text{-}tot,out}$ =570 nVrms	

3) *Second Stage: LP Filter*

The output signal from the OCP block undergoes the filtering operation as provided by the LP Filter (Figure 1). Specifically, the low-pass filter implemented for the application is a 4th order Sallen-Key filter. The filter is responsible for reducing high-frequency noise, also acting as an anti-aliasing filter. The Sallen-Key topology was chosen to provide a unity gain and a low output impedance. The 4th order filter consists of two second-order stages designed as a cascade of a Bessel (Q_1 = 0.56) and a Chebyshev filter (Q_2 = 1.305) [10].

The unity gain design was achieved by setting the cutoff frequency (f_c) to 200 Hz, and the quality factors (Q_1 and Q_2), thus, parametrizing the ratios between the resistors and capacitors involved in the Sallen-Key topology. The obtained values were then modified and adjusted in accordance with some specific recommendations for COTS implementations: (i) using capacitors greater than 10 pF; (ii) using stable capacitor dielectrics like C0G(NP0); (iii) using SMD components with a 1% (max) tolerance. Figure 4.a shows the implemented circuit.

The op-amps U4 and U5 in Figure 4.a are MAX4477, like the differential stage of the OCP, operating on a single supply of +3.3V. Figure 4.b shows a comparison between the Bode diagram measured by the implemented board and that simulated using OrCAD PSpice software. The reported experimental results show a real cutoff frequency of 195.6 Hz against 199.52 Hz from simulation.

In terms of noise budget estimate, under the same condition in Table 1, the total noise given by OCP (3 op-amps) + LP Filter is about 2.28μVrms. This noise level allows the use of ADCs with up to 18 bits of resolution, considering a full-scale voltage (V_{FS}) of 3.3V [10].

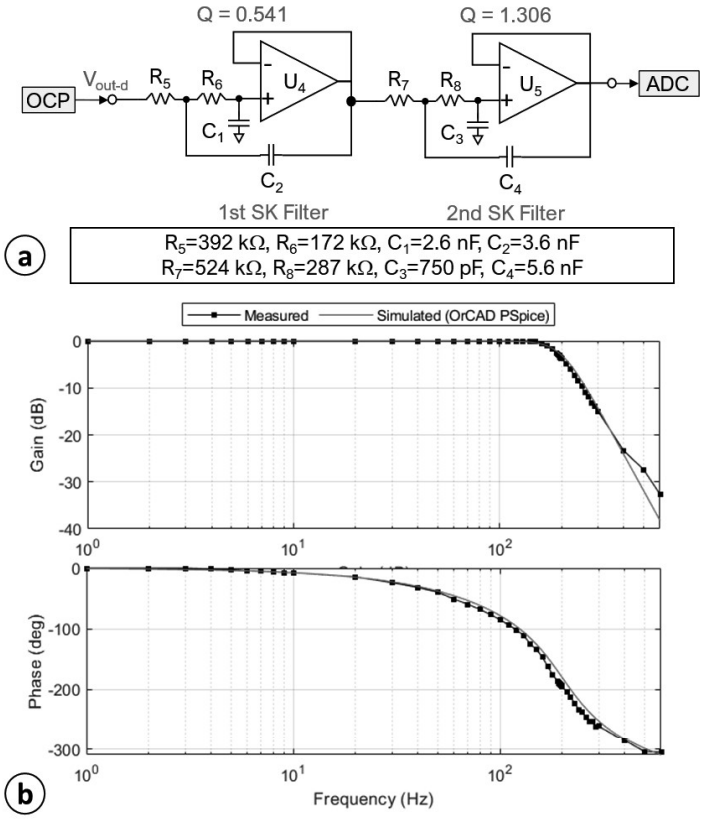

Fig. 4. LP Filter. (a) 4th-order Sallen-Key filter with components value; (b) Comparison between measured and simulated (OrCAD PSpice) Bode Diagram of the implemented 4th-order LP Sallen-Key filter.

4) *Digital Section*

Microcontroller. The proposed system uses as microcontroller (μC) block in Figure 1 the NINA-B306 by u-blox. The NINA-B306 is a stand-alone Bluetooth 5 low-energy module that optimizes its form factor (10 mm × 15 mm) embedding a patented Abracon PCB antenna in addition to the

nRF52840 microcontroller. Figure 5 summarizes the main features of the module selected for the presented application.

Among the main features of the NINA-B3 module, it is possible to find the inclusion of the nRF52840 chip, which embeds an Arm Cortex M4 with FPU processor operating at 64 MHz. The nRF52840 has 1 MB of flash and 256 kB of RAM for code and data storage.

The nRF52840 features an 8-channel Successive Approximation Register (SAR) ADC with 12-bit resolution and a 200 ksps of maximum sampling rate.

The ADC resolution can be increased up to 14 bits by enabling the oversampling. The ADC incorporates an automatic calibration procedure to compensate for gain and offset errors. Registers setting also permits dynamic selection of the ADC reference voltage between V_{DD} (and related divisors) and stable internal references.

In terms of power efficiency, the NINA-B3 can power down different sections of the module when not needed, managing three main working modes: (i) active, (ii) standby, and (iii) sleep. Sleep mode is the deepest power-saving mode since almost all functionalities are stopped. The standby mode (less efficient than sleep mode) powers down the module while keeping configurations and RAM intact.

To manage these different power-saving modes, for the proposed application, an analog function GPIO has been set to route a low-power (LP) comparator. Also, an NFC antenna connector has been provided on board and routed to the NINA-B3 dedicated ports.

Finally, the nRF52840-embedded Real Time Counter (RTC) is employed to generate scheduled interrupts.

Waking up the NINA-B3 from sleep mode relies on external events such as NFC field detection or voltage on LP analog comparator pins (kept active in sleep mode).

The standby mode can be interrupted the RTC, NFC, and LP comparator. During standby mode, the module is clocked at 32 kHz, generated by an internal 32 kHz crystal oscillator (Figure 5).

The management of the module's operating modes is entrusted to the Sweat Test Control firmware as explained in Sec. II.B. Data transmission is handled by the Abracon PCB antenna, which operates at 2.4 GHz (40 channels) with a radiated output power up to +10 dBm.

The supported radio modes at 2.4 GHz are Bluetooth Low Energy (BLE) and IEEE 802.15.4 with data rates ranging from 125 kbps to 1 Mbps.

DAC. As shown in Figure 5, the microcontroller connects via SPI, the LTC2611 DAC from Linear Technology, to manage the V_{OS} voltage as shown in Figure 3 and Section II.A.2. The LTC2611 is a low-power rail-to-rail output 14-bit resolution DAC. The device can be software-controlled to enter in power-down mode, reducing the consumption from approximately 300 µA to 1 µA (max). The DAC ensures low noise level on the buffered output achieving 15 µVpp (0.1-10 Hz) of noise with an offset <1.5 mV.

5) *Power Section*

The FlexPCB is powered by a rechargeable lithium-ion coin battery LIR2477 (24 mm ⌀, h: 7.7 mm) with a nominal voltage of 3.7V and a capacity of 200 mAh. The voltage from the power source is used as the input voltage for a Low-Dropout Regulator

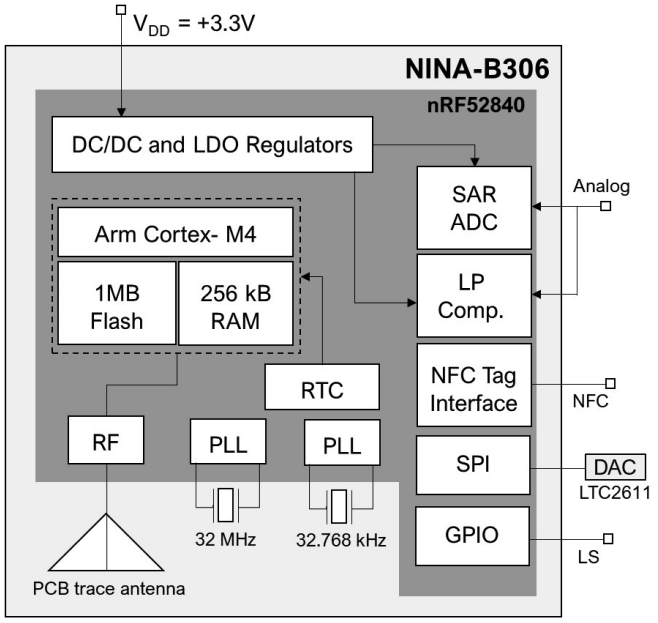

Fig. 5. Schematic representation of NINA B306 features of interest.

(LDO), specifically the BU33SD5WG by Rohm, and as the bias voltage for a load switch, the TPS22975 by Texas Instruments. The employed LDO has a maximum dropout voltage of 85 mV for the considered voltages, allowing for a functional reduction from 3.7 V to 3.3 V. Optimal load regulation ensures an output of 3.3V (±6 mV) up to output currents of 500 mA. The device consumes between 51 µA and 62 µA when considering a V_{IN} of 3.7V and an output current in the range of 50 mA to 100 mA.

Downstream of the LDO, there is the load switch TPS22975, whose purpose is to disable the power supply to the OCP and LP Filter analog chain when measurements are not needed. The device receives 3.7V from the battery as V_{BIAS} and 3.3V from the LDO as V_{IN}. The enabling line for transmission to the power delivery network is managed by a microcontroller GPIO and coordinated by the firmware. The time required for control adjustment is approximately 2.2 ms (soft start compatible with the analog conditioning chain's requirements), while power cutoff occurs in about 3 µs.

B. *Sweat Test Controller*

The microcontroller runs a firmware, named Sweat Test Controller in Figure 1, which has multiple functions: (i) manages acquisitions from the analog read-out circuit; (ii) processes acquired data to derive the concentration of the target ion (Cl^-); (iii) transmits acquired data to the doctor via FHIR server; (iv) suggests genetic tests in case of potential detection of a pathology; (v) schedules measurements based on the therapy; (vi) manages the power consumption of the board.

Figure 6 provides an overview of the main functionalities of the Sweat Test Controller in the form of a flow chart.

Initialization. In its initial operational mode, the proposed system can be switched from a sleep state (System OFF) to a wake-up state (System ON) through the following actions: (i) inserting the battery (first time after programming session); (ii) touching a designated pad on the bottom of the board (LP Comparator) when battery is inserted; (iii) powering an NFC antenna for additional data exchange.

Differently, in its nominal operational mode, the system is

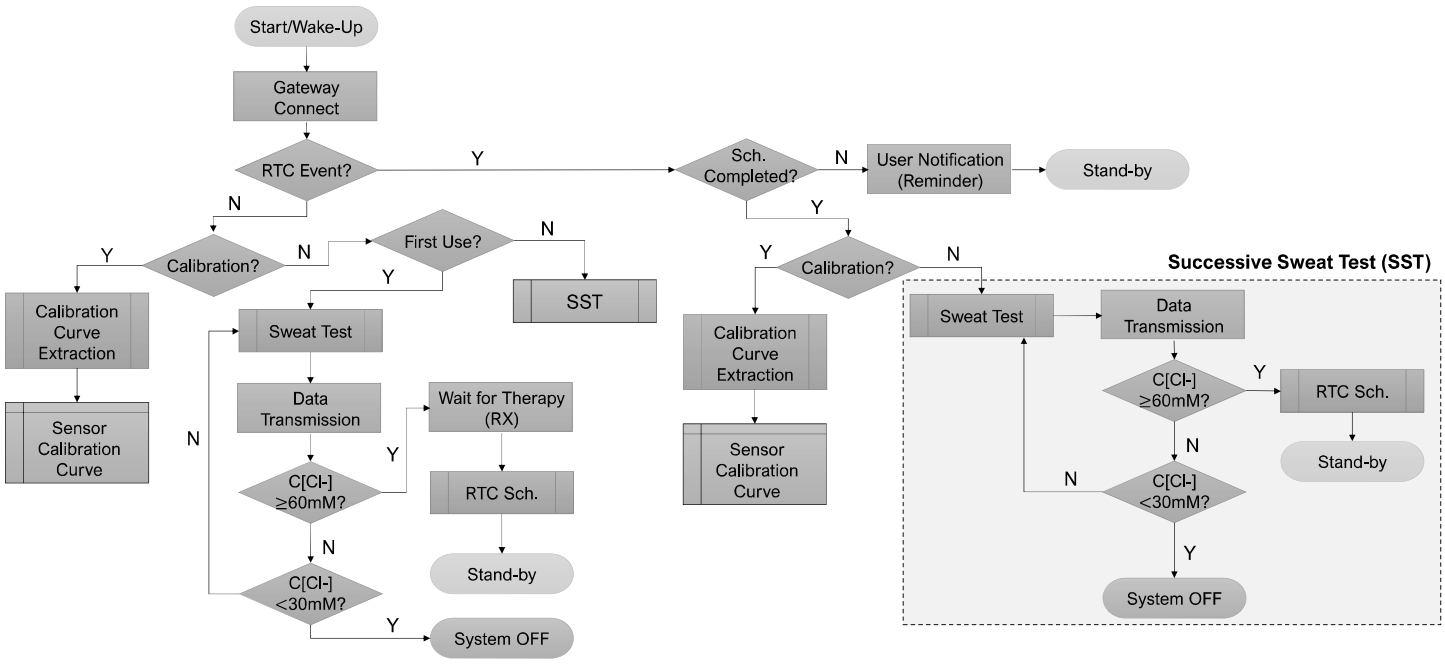

Fig. 6. Simplified flow-chart of implemented Sweat Test Controller firmware

typically in a stand-by state. In addition to the above-mentioned events, the occurrence of an RTC event can also bring the system to a wake-up state from stand-by one. This mode is used in the case of scheduled tests or voluntary measurements.

Once brought into an active state, the device connects via BLE to the designated portable gateway (in our application, a smartphone).

Subsequently, following the flow chart in Figure 6, the system first verifies the wake-up event source through a dedicated register ("RTC Event?" – Figure 6). If the event was not triggered by the RTC, the wearable Sweat Analyzer sends a Bluetooth message to the portable gateway, in order to enable the user to choose between *calibration* and *measurement*.

Calibration Curve Extraction. In the case of a calibration request, the system will initiate the procedure identified as Calibration Curve Extraction in Figure 6. This procedure allows the proposed device maximum flexibility in terms of the electrochemical sensor to be used for measurement.

Indeed, once a sensor of interest is identified, it can be connected to the board through the provided Molex connector (an adapter is required).

With the electrode in place, the first step is to specify, through the dedicated application on the portable gateway, the concentration, in millimolar (mM), of the target ion, considering the calibration solution to be measured. Subsequently, a drop of this solution can be deposited within the sensing area between the RE and the WE connected to the OCP stage.

Starting the measurement, the Sweat Test Controller drives the load switch to power the analog section of the board. After 10 ms, the SAR ADC will begin sampling at a resolution of 14 bits and a sampling frequency (f_s) of 1 ksps. Only one average value per minute is included in the resulting dose-response curve. The acquisition can be manually interrupted or automatically if, within 5 minutes, the acquired data does not deviate more than ±2 mV from the average. The point to be included in the calibration curve is derived from the average of these last 5 samples. The procedure is repeated for all concentrations deemed useful in defining the calibration curve.

Upon completion of the acquisition, the microcontroller will drive the load switch cutting off power to the analog section.

Once all the points of interest are obtained, the Sweat Test Controller extracts a logarithmic trend curve, whose slope in log-linear scale (a straight line) determines the sensitivity of the calibrated sensor, expressed in millivolts per decade of concentration (mV/dec[C(Cl^-)]).

The equation of the trend curve (Sensor Calibration Curve in Figure 6) is stored and can be used during the measurements to convert a voltage reading into the corresponding target ion concentration.

Sweat Test. If a measurement is requested, the Sweat Test Controller will check for previous acquisitions or the past uploading of a therapy into memory. In the case of a first-time use, the system will await initiation request from the user.

Once measurement is started, the Sweat Test Controller drives the load switch to power the analog section of the board. As reported for the calibration procedure, after 10 ms, the SAR ADC will begin sampling at a resolution of 14 bits @ f_s = 1 ksps. Only one average value per minute is examined. The acquisition is automatically terminated if, within 5 minutes, the acquired data do not deviate from each other by more than ±2 mV. The measured voltage value is extracted from the average of these last five samples. Upon completion of the acquisition, the microcontroller will drive the load switch to cut off power to the analog section.

The stored calibration curve, is obtained applying the Nernst Equation:

$$E = m \cdot \log_{10}(a[Cl^-]) + q \quad (1)$$

to correlate the measured voltage with the concentration of the

target ion in solution. In Equation (1), E is the voltage value, m is the sensitivity of the calibrated sensor expressed in mV/dec, $a[Cl^-]$ is the activity value of the target ion, and q is the intercept of the line in the log-linear domain. The activity of the target ion can be considered equal to its concentration $C[Cl^-]$, assuming weakly concentrated solutions,

From equation (1), the concentration of the target ion is derived based on the measured voltage value, $\hat{E}$, as follows:

$$C[Cl^-] = 10^{\frac{\hat{E}-q}{m}} \quad (2)$$

Test Outcome Assessment. Once extracted, the estimated value is transmitted via BLE to the gateway, which will create an observation on the FHIR server using a post operation with the device's own software agent token. The Data Transmission routine is outlined in the form of a sequence diagram in Figure 6. Following the transmission of the test result, the Sweat Test Controller verifies whether the value of C[Cl^-] falls within specific physiological ranges of interest.

If C[Cl^-] < 30 mM, the subject can be considered healthy, and the system will be permanently switched off (System OFF). In this case, the system will need to be reprogrammed by modifying the patient's parameters for reuse.

If C[Cl^-] ≥ 60 mM, the subject is considered potentially affected by cystic fibrosis, as the sweat test was arranged following an Immunoreactive Trypsinogen (IRT) test. In this case, the system will initiate the routine called Wait for Therapy in Figure 6. This routine, represented as a sequence diagram in Figure 7, illustrates that the system sends a suggestion for specific genetic tests to the doctor ("sugg" in figure 7), based on which a specific therapy will need to be defined.

The system remains in a state of waiting to receive a therapy file ("thpy" in Figure 7) that the doctor will update through the dashboard. Then, the therapy file will be made available on the server through the "get" function (i.e.: get("thpy") in Figure 7). Once received, the gateway forwards the therapy to the sweat analyzer.

Based on the received data, the Sweat Test Controller sets a sequence of RTC events (RTC Scheduling in Figure 6).

These events will serve to update a countdown on the portable gateway application (User Notification). Upon completion of the update, the system is put into standby until the occurrence of a new wake-up event. Once the scheduling is completed (Sch. Completed in Figure 6), it will be necessary to proceed with the pharmacological compliance check as requested by the therapy. In this case, the application on the gateway will unlock the possibility to request calibration or a *scheduled* Sweat Test. The Sweat Test will be conducted as previously described (Successive Sweat Test is indicated as "SST" in Figure 6).

At the end of the test, if C[Cl^-] still exceeds 60 mM, the system will reschedule the RTC for the subsequent verification, placing the system in standby mode, awaiting a new wake-up event. In all cases, if the Sweat Test routine returns a concentration value within the intermediate range, it will be defined as borderline, and the measurement will be repeated following the procedures listed above.

Offset Compensation. The proposed sweat analyzer provides a routine for managing the offset voltage (V_{OS}). To calibrate the V_{OS}, it is necessary to short-circuit both the inputs of the WE and RE to ground using the switch on the board.

The Sweat Test Controller will communicate with the DAC via SPI, driving it to provide the needed dc value of 1.65 V (as in Figure 3), centering the AFE output signal within the dynamic range of the ADC (V_{FS}=+3.3V). The microcontroller will then control the load switch to turn on the analog chain and begin the acquisition of 5000 samples with a resolution of 14 bits at a sampling rate of 1 ksps.

The average number of LSBs from $2^N/2$ is used to correct the offset using the DAC. The DAC is also used for dynamic shifting of signal centering in the case of V_{FS} changes at run-time.

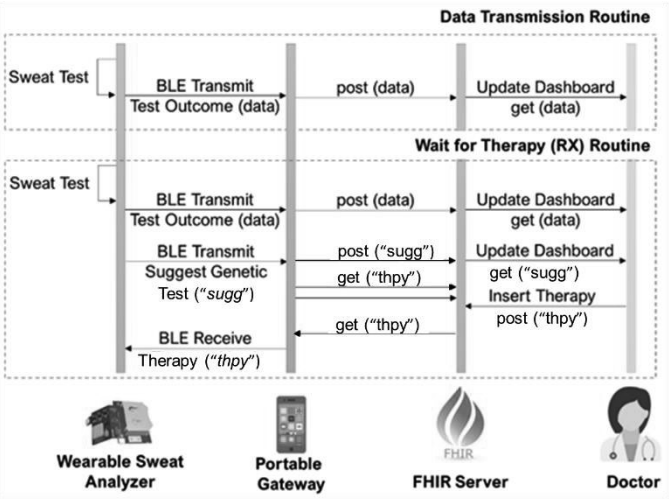

Fig. 7. Transmission Data and Wait for Therapy Routine sequence diagrams.

C. The Electrodes

The wearable sweat analyzer exploits potentiometric technique for chloride detection, by measuring the potential difference between the WE and RE, when a sweat sample or a solution containing chloride ions is drop-casted over the electrodes.

The electrodes realized for this application are based on the technique introduced in our previous work [11]. Respect the ones in [11], the here proposed electrodes differ in terms of their geometry and RE passivation methodology. Figure 8.a illustrates the geometry of the electrode pair that was designed, realized in bendable material and characterized. Figure 8.b provides a snapshot of the electrodes, demonstrating their flexibility.

To realize the electrode pair, two silver traces with the geometry in Figure 8.a were made by depositing silver ink on 75 µm of Mylar substrate. After air drying for 5 minutes at room temperature, the deposited silver underwent a curing phase using a constant airflow heating profile (volumetric flow rate = 50 l/min), maintaining a temperature of 100°C for 10 minutes. This latter procedure has been proven to be effective in improving the ink adhesion to the substrate.

The WE is made of Ag/Ag+ and is left unmasked for all the technological steps. The RE is prepared by masking the contacts (pads) with removable insulator and immersing the unmasked silver trace in sodium hypochlorite. The immersion lasts for 10 seconds. Once removed, the sodium hypochlorite is left to act in still air for 15-20 seconds. The procedure realizes a thin layer of passivating silver oxide (Ag_2O) that stabilizes the RE (darker area in Figure 8). Compared to the geometry reported in our previous work [9] where the passivation of the

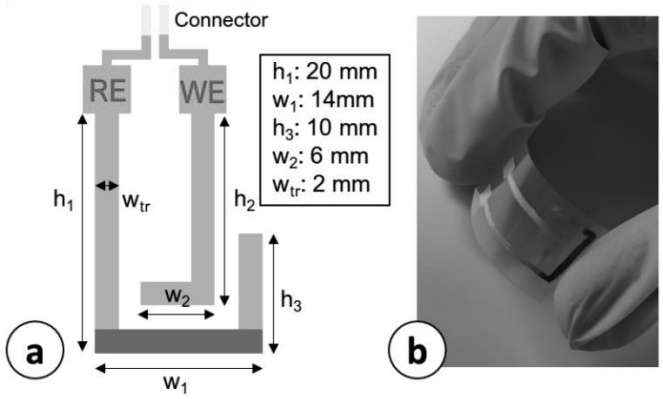

Fig. 8. Proposed Electrodes. (a) Geometry; (b) Electrodes snapshot

RE was done by drop-casting, the new geometry allowed to perform the oxidation step by controlled immersion of the RE in sodium hypochlorite, improving stability of the sensing area. To stop the reaction, the RE is rinsed with deionized water. The new geometry demonstrated to be suitable for handling the rinsing step removing the sodium hypochlorite from the RE without affecting WE. The morphology and chemical composition of silver ink has been investigated by Scanning Electrode Microscope (SEM) [10]. In particular, the Energy Dispersive X-ray Spectroscopy (EDS) demonstrated that the used silver ink has 99%. of purity.

To test the capability to detect different Cl^- concentrations, a set of 5 different solutions, each, with different NaCl concentrations have been used to draw the calibration curve. Between every drop-cast the previous solution has been rinsed using deionized water and has been allowed to dry at room temperature for about a few seconds. At each measurement, the concentrations were increased from 1mM to 10 mM, 50 mM, 75 mM and 100 mM.

Figure 9.a shows an excerpt of the dose-response curve of the proposed electrodes, limited to the range relevant for our application, which is from 50 mM to 100 mM. The ΔV (V_{WE}-V_{RE}) drop, expressed in millivoltt, corresponds to the concentrations C[Cl^-] in solutions of NaCl at three different concentrations (50 mM, 75 mM, 100 mM).

The repeatability of the measurements (or stability of the system) has been proved by keeping measuring the same concentration for 10 minutes. We assume that the stability is reached when the possible oscillation over the average value are below +/-2mV. Some of the measurement results are shown in Figure 9. The dose curve (figure 9.a) indicates that for each concentration the stability (i.e. less than +/-2mV over the averaged value) is reached in 5 minutes from the starting acquisition. After that, the plateau hold for the remaining 5 minutes, and it is shown in figure 9.a by 5 points made as average over 60 measurements (one measurement per second per minute).

This means that the signal detection will be considered stabilized if the potential has not variation within [-2mV – 2mV], in the last 5 minutes. So, if the potential variation is within [-2mV – 2mV], the measurement is stable. The red curve is the one extracted from our measurement setup, while the dashed black curve is the comparative one, obtained by extracting voltage values every second, rather than the average of 60 seconds every minute as described in Sec. II.B.

In our measurements the deviation during the 5 minutes plateau are on all steps of the calibration curve ranges from 0.4 mV to 0.3 mV, well below the ±2mV.

Figure 9.b shows the calibration curve of the sensor for same range of NaCl concentrations of Figure 9.a (i.e., 50 mM, 75mM and 100 mM). The observed slope of the calibration curve (figure 9.b) is 56.9 mV/dec.

Additional measurements have been carried out to get the Cl^- concentration in 10mM and 5mM of solution (not shown because the range is not of interest for the application here investigated). Using the proposed electrodes and considering the statistical Shapiro-Wilk method [12], given an accuracy of ±2mV over the WE voltage referred to the RE one, the deviation on the Cl^- concentration from the calibration curve for 100 mM of NaCl solution (worst case) is ±3.4 mM. The deviation is improved to ±2.1 mM around 50 mM of NaCl, and further upgrades to ±0.6 mM at 10 mM of NaCl concentration. It can be underlined that reducing the solution concentration, the accuracy improves to ±1mV which means that the equipment avoids the occurrence of false positive being more accurate in low concentration solution.

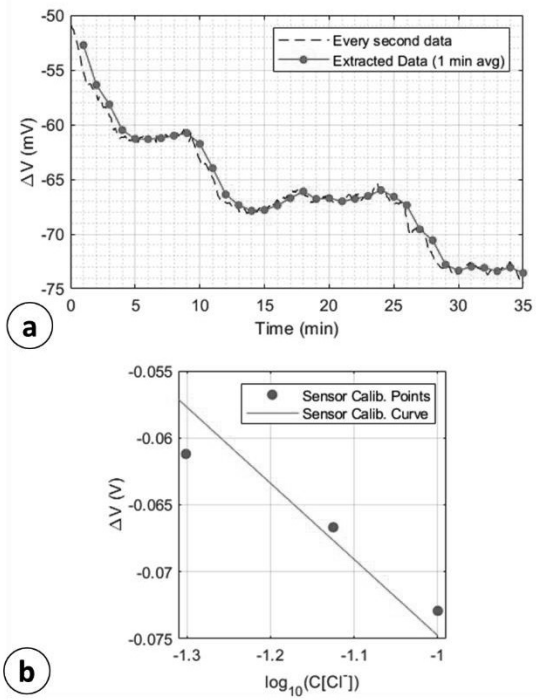

Fig. 9. Electrodes Calibration. (a) Dose response curve and (b) Extracted Calibration Curve limited to the pathological range {50 mM - 100 mM}. Data extracted with the proposed electronics.

III. Power Consumption

The proposed sweat analyzer has two main operating modes: (i) active measurement and (ii) standby with RAM retention. The currents drawn by the devices are distributed as follows:

1. Stadio OCP – ON: 64 μA (worst case), OFF: 0;
2. MAX4477 (LP Filter) – ON: 2.2 mA; OFF: 0;
3. NINA-B3 – Active: 2.8 mA; Stand-by (RAM retention): 1.3μA; TX (+8dBm): 14mA (peak)
4. LTC2611 (DAC) – ON: 298 μA, OFF: 1μA;
5. BU33SD5WG (LDO) – ON: 62 μA
6. TPS22975 (Load Switch) – ON: 38 μA

Considering a standard time interval of 1 hour of operation, during the first mode (i.e., active measurement), the analog chain is activated for approximately 20 minutes (INA333 + MAX4477), the NINA-B3 is active for 20 minutes, followed by data transmission to the portable gateway, then goes in standby mode for the remaining ~40 minutes. The DAC is active for 20 minutes and then turns OFF for the remaining 40 minutes. The LDO and Load Switch, however, remain active. The average current consumption in this configuration is approximately 1.78 mA.

The standby mode (second operational mode) involves only the NINA-B3 module in standby mode, the DAC in the same mode, and the LDO and Load Switch, which remain active. The average power consumption in this mode is ~100 µA.

Considering a 3.7V LIR 2477 battery with a capacity of 200mAh, as described in Section II.A.5, and considering the described profiles, the estimated battery life for the proposed device is 82 days (average consumption of the device: 350 µW). Further perspectives consider the sweat production being stimulated by an integrated heater [13] (on the opposite side respect the electrodes) to reach around 25°C and keep the same temperature for 10 minutes. From [13] it is possible to evaluate the power consumption of the heater of about few tens of mW (i.e. around 20mW).

IV. Case Study

John, a fictional name used for privacy, is a six-year-old boy. When two-month-infant, John underwent an Immunoreactive Trypsinogen (IRT) test, which yielded a positive result. In accordance with the dedicated guidelines, John underwent a sweat test through outpatient sampling. The sweat sample was analyzed by a specialized laboratory, which returned a chloride concentration in the sweat of approximately 80 mM. This value falls within a pathological pattern typical of cystic fibrosis.

At the age of 6, John can begin dedicated therapy. This will involve the need to conduct a new sweat test and schedule a series of measurements to verify the effectiveness of the medication until the test becomes negative ($C[Cl^-] < 30$ mM).

John is recruited for the validation of the proposed device and is called in for a visit with his parents.

Initialization. During the outpatient visit, the doctor enters the patient's data through the dashboard on the FHIR server, enabling the sweat analyzer application on a portable gateway (parent's smartphone).

The software agent on the portable gateway receives authorization credentials from the FHIR server, that will be used to post data at the time of observation.

The FlexPCB is fixed by means of a bracelet on the boy's forearm and brought to a wake-up state through the pressure of the skin on the pad connected to the LP comparator.

The default portable gateway connects Sweat Analyzer via BLE through standard pairing.

Sweat Test. As reported in Sec. II.B, once connected, the application allows the user to choose between sensor calibration and conducting the sweat test. Since previously characterized electrodes are used (calibration curve is already stored in the device) no further calibration will be necessary. Figure 10.b shows an example of sensor calibration curve ranging from 1 mM to 120 mM extracted by the proposed system (orange line).

Therefore, the test is started by remotely initiating the measurements (via application). The microcontroller will be responsible for powering the analog section, and after 10 ms, it will begin with the acquisitions as described in the Sweat Test paragraph (Sec. II.B). Figure 10.a shows a response curve obtained through experimental measurements. The curve stops at 14 minutes because the device automatically halted data acquisition, as the average calculated at the 14th minute did not deviate by ±2 mV (black dashed lines - Figure 10.a) from the measurements of the last 5 minutes (red markers - Figure 10.a).

The calculated average voltage is 59.11 mV, which, when converted to chloride concentration $C[Cl^-]$ using Eq.(2), corresponds to 70.92 mM. This value, represented as a red marker along the calibration curve in Figure 10.b, falls within the pathological range determined by the blue dashed limit of 60 mM.

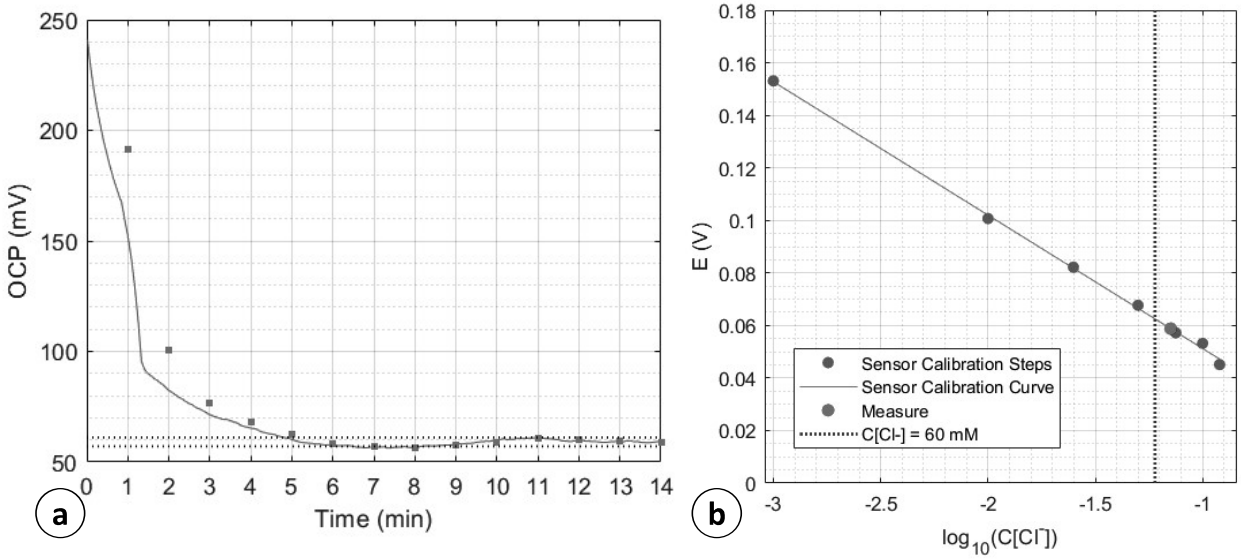

Fig. 10. Experimental measurements. (a) Response curve with acquired values (blue line), computed values (red marker) and settling boundaries (black dahed lines); (b) Sensor Calibration Curve with calibration steps, extracted log-linear fitting (Calibration Curve), extracted measure and pathological limit ($C[Cl^-] = 60$mM).

Diagnostic Support. Since this is the first measurement conducted with the proposed device, the Sweat Test Controller sends the data to the portable gateway to populate the observation body .json for posting to the FHIR server used by the facility. The code below represents the observation body. json, where `valueCl_Double` is the derived chloride concentration value, and the `Suggestion` field summarizes the specific diagnostic suggestion to the physician to proceed with a check for the 2nd class ΔF508 mutation. Once this message is sent, the Sweat Test Controller puts the microcontroller in standby mode with scheduled wake-ups every 2 hours. At each wake-up phase, a flag is sent to the gateway to proceed with a GET request for the genetic test result from the FHIR server.

Code: Example Observation Body .json
no Header for post on FHIR server is included

```
{
  "resourceType": "Observation",
  "status": "final",
  "category": [
    {
      "coding": [
        {
          "system": "http://***/sct",
          "code": "******",
          "display": "Signs/Cl_measure/surveillance "
        }
      ]
    }
  ],
  "code": {
    "coding": [
      {
        "system": "http://***/sct",
        "code": "****",
        "display": "C[Cl-] measurement"
      }
    ]
  },
  "subject": {
    "reference": "Patient/(**Fiscal Code from get**)"
  },
  "effectiveDateTime": "yyyy-mm-ddThh:mm:ss+02:00",
  "performer": [
    {
      "reference": "Patient/114"
    }
  ],
  "valueCl_Double": 70.92
  "Suggestion": "Suggested genetic test for deltaF508
Mutation"
}
```

Scheduled Therapy Surveillance. Once the therapy is received, along with associated pharmacological monitoring intervals (e.g., M0, M1, M3, M6, M12, +M6 after M12), the Sweat Test Controller sets the RTC scheduling to send updates to the portable gateway twice a day with a countdown before the next measurement. Subsequently, it enters standby mode until the scheduled RTC event, in accordance with the description in Sec. II.C. From this moment onwards, tests can be conducted at home following the same steps as during the outpatient visit. Figure 11 shows an example of therapeutic monitoring over the course of 18 months. In this specific case, during the first 3 months, the values consistently exceeded the pathological threshold of 60 mM, leading to a rescheduling of the RTC (therapy). At M6, the measurement returned an intermediate value of 50.93 mM. This value was categorized as borderline, and a new measurement was scheduled 2 hours later. The repeated measurement returned a value higher than 60 mM.

At M12, the same ambiguous situation occurred again. The second measurement yielded a value below 30 mM. However, the system does not interrupt the monitoring for repeated measurements unless there is direct medical intervention. At M18, with a concentration of 23.16 mM, John returned negative outcome for the sweat test. There will no longer be a need for continued monitoring. The system will lead to System OFF mode as described in Sec. II.C.

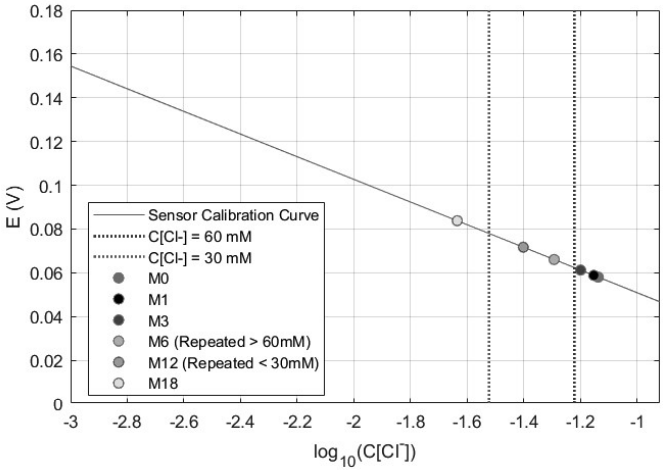

Fig. 11. Example of follow-up for scheduled therapy surveillance

V. Conclusions

A miniaturized, flexible and wearable system for conducting sweat tests, even in home environment, has been designed and characterized. The key breakthroughs of the proposed device include: (i) faster test execution compared to current gold standards; (ii) simplified sweat sample acquisition phase; (iii) automatized sweat test procedure; (iv) improved portability of the electronics used for potentiometric measurements and data analysis; (v) the capability of storing data with AI-based reasoning systems capable of self-calibrating data interpretation, based on factors related to the environment, test execution timing, and patient history; (vi) capability to acquire, process and transmit test outcomes and diagnostic support to specialized medical centers in real-time.

The proposed system features compact electronics (only 49.4 mm × 39.5 mm) on a flexible PI substrate. The electronic device enables potentiometric detection of Cl^- concentration by measuring the potential difference between electrodes fabricated on flexible, replaceable, and biocompatible plastic substrate. The resolution guaranteed by the electronics is of ± 0.805 mV, increased to a conservative ± 2 mV at the firmware level in order to be able to manage the electrodes adjustment. This value is programmable and can be reduced, improving the system resolution. The conservative variation of ± 2 mV corresponds, in the worst case, to a sensing resolution of ±3.4 mM. The sensitivity achieved by the electrodes is 56.9 mV/dec from 5 mM to 100 mM.

The whole device average power consumption is of 350 μW, guaranteeing a continuous operation of approximately 3 months with a 200mAh capacity LIR battery.

These results are in compliance with resolutions achieved by specialized medical equipment, opening the possibility of using this system to reduce costs, execution times, and ensuring continuous monitoring of CF patients.

REFERENCES

[1] K. K. Yeung, T. Huang, Y. Hua, K. Zhang, M. M. F. Yuen, e Z. Gao, «Recent Advances in Electrochemical Sensors for Wearable Sweat Monitoring: A Review», IEEE Sens. J., vol. 21, fasc. 13, pp. 14522–14539, lug. 2021, doi: 10.1109/JSEN.2021.3074311.

[2] H. Luo e B. Gao, «Development of smart wearable sensors for life healthcare», Eng. Regen., vol. 2, pp. 163–170, 2021, doi: 10.1016/j.engreg.2021.10.001.

[3] I. N. Hanitra, F. Criscuolo, S. Carrara, e G. De Micheli, «Multi-Target Electrolyte Sensing Front-End for Wearable Physical Monitoring», in 2019 15th Conference on Ph.D Research in Microelectronics and Electronics (PRIME), Lausanne, Switzerland: IEEE, lug. 2019, pp. 249–252. doi: 10.1109/PRIME.2019.8787768.

[4] J. F. Cheng, J. C. Chou, T. P. Sun, S. K. Hsiung and H. L. Kao, "Study on a multi-ions sensing system for monitoring of blood electrolytes with wireless home-care system", IEEE Sensors Journal, vol. 12, no. 5, pp. 967-977, 2012.

[5] W. Gao, S. Emaminejad, H. Y. Y. Nyein, S. Challa, K. Chen, A. Peck, et al., "Fully integrated wearable sensor arrays for multiplexed in situ perspiration analysis", Nature, vol. 529, no. 7587, pp. 509-514, 2016.

[6] J. V. Pagaduan, M. Ali, M. Dowlin, L. Suo, T. Ward, F. Ruiz, et al., "Revisiting sweat chloride test results based on recent guidelines for diagnosis of cystic fibrosis", Practical Laboratory Medicine, vol. 10, pp. 34-37, 2018.

[7] Guidelines for the performance of the sweat test for the investigation of cystic fibrosis in the UK 2nd version (these guidelines supersede the 2003 guidelines) an evidence-based guideline; March 2014

[8] Cirilli N, Raia V, Rocco I, De Gregorio F, Tosco A, Salvadori L, Sepe AO, Buzzetti R, Minicuci N, Castaldo G. Intra-individual biological variation in sweat chloride concentrations in CF, CFTR dysfunction and healthy pediatric subjects. Pediatr Pulmonol 2018;1-7

[9] A. J. Bard e L. R. Faulkner, Electrochemical methods: fundamentals and applications, 2. edition. New York Weinheim: Wiley, 2001.

[10] D. De Venuto, G. Mezzina, A. Tricase, P. Bollella, G. Mascellaro and L. Torsi, "Wearable and Flexible Fibrosis Cystic Tag with Potentiometric Chloride Activity Sensing," 2023 9th International Workshop on Advances in Sensors and Interfaces (IWASI), Monopoli (Bari), Italy, 2023, pp. 115-120, doi: 10.1109/IWASI58316.2023.10164336.

[11] De Venuto, D., De Venuto, D., Mezzina, G., Mascellaro, G., Torsi, L. (2024). Chloride Activity Sensing in Sweat for Cystic Fibrosis Diagnosis by Biocompatible Flexible Tag. In: Ciofi, C., Limiti, E. (eds) Proceedings of SIE 2023. SIE 2023. Lecture Notes in Electrical Engineering, vol 1113. Springer, Cham. https://doi.org/10.1007/978-3-031-48711-8_16.

[12] King, Andrew P., and Robert Eckersley. Statistics for biomedical engineers and scientists: How to visualize and analyze data. Academic Press, 2019.

[13] Nicola Lovecchio, Valentina Di Meo, Domenico Caputo, Augusto Nascetti, Alessio Crescitelli, Emanuela Esposito and Giampiero de Cesare, "Transparent Oxide/Metal/Oxide Thin Film Heater with Integrated Resistive Temperature Sensors", IEEE Sensors Journal, vol. 21, issue 17, pp. 18847-188.